APPLIED GEOPHYSICS, Vol.8, No.3 (September 2011), P. 163 - 170, 7 Figures.
DOI: 10.1007/s11770-011-0293-1

# Analyzing the mid-low porosity sandstone dry frame in central Sichuan based on effective medium theory

Yan Xin-Fei[1,2], Yao Feng-Chang[1,2], Cao Hong[1,2], Ba Jing[1,2], Hu Lian-Lian[3], and Yang Zhi-Fang[1,2]

**Abstract**: Tight gas sandstone reservoirs in Guang'an are characterized by wide distribution and low abundance. Sandstone samples from this area usually have low porosity and poor connectivity. We analyze the observed velocity data of tight sandstone samples with the Mori-Tanaka model, and give the sandstone framework physical model in this area based on theory and experiment analysis. The matrix modulus was obtained by an empirical relationship and then the experiment data were compared with the values predicted by the Mori-Tanaka model with different pore shapes. The results revealed that the experiment data were close to the model with low pore aspect ratio. Considering the matrix modulus and pore shape variation, we find that, under the condition of small mineral composition change, the effective pore aspect ratio of these samples increased with porosity evidently.
**Keywords**: tight sandstone, dry frame, Mori-Tanaka model, pore aspect ratio, inclusion

## Introduction

Along with society's growing demand for oil and gas resources and increasingly exhausted conventional oil and gas resources, people put more attention to unconventional oil and gas resources, such as oil sands, oil shale, tight sandstone gas, shale gas, and so forth. In China, there are widely distributed tight sandstone reservoirs with the gas reserves occupying a large proportion of the total gas reserves (Zhu et al., 2009). Rock physics models can link reservoir parameters and elastic parameters together (Mavko et al., 1998), which is very important for researches in seismic inversion and interpretation, acoustic logging, laboratory core measurements, and so on.

The Xujiahe formation sandstone reservoirs in Guang'an area are typical of tight sand with low porosity and permeability or even ultra-low porosity and permeability. Because of these characteristics, according to the opinion of Vernik and Kachanov (2010), these sandstones can be described microstructurally as a continuous material with isolated pores and intergranular cracks. So we adopted the inclusion-based effective medium model to analyze tight sandstone experimental data from Guang'an.

Four inclusion-based effective medium models are discussed in the literature (Mavko et al., 1998; Kachanov et al., 1994; Berryman et al., 1996; Berryman and Berge, 2006), including the self-consistent model (SC), Kuster-Toksöz model (KT), Mori-Tanaka model (MT) and differential model (DEM). Self-consistent

Manuscript received by the Editor March 15, 2011; Revised manuscript received June 21, 2011.
*This research is supported by the National Natural Foundation of China (No. 41104066), the Basic Research Programs of CNPC during the 12th Five-Year Plan Period (No. 2011A-3601), the Major State Basic Research Development Program of China (No. 2007CB209505), and RIPED Young Innovation Foundation (No. 2010-A-26-01).
1. Research Institute of Petroleum Exploration and Development, Beijing 100083, China.
2. Key Laboratory of Geophysics, PetroChina, Beijing 100083, China.
3. China University of Geosciences (Beijing), Beijing 100083, China.

schemes were firstly developed by Hill (1965) and Budiansky (1965) based on strain energy which was original proposed by Eshelby (1957). Hill's model (1965) is only valid for spherical inclusions, so Wu (1966) further developed the self-consistent model for ellipsoidal inclusions. Korringa et al. (1979) formulated their self-consistent model which was suitable for multiphase media. Based on elastic wave scattering theory, Berryman (1980) established another self-consistent scheme for estimating the effective elastic parameters of a medium with ellipsoidal inclusions. Based on first order long wavelength scattering theory and taking the effect of inclusion properties, volume fraction and shape into account, Kuster and Toksöz (1974) formulated their theoretical model for calculating effective properties in two phase media, which is the well known Kuster-Toksöz model. For a medium with inclusions, Mori and Tanaka (1973) proposed an average stress field approximation scheme which was widely used in the engineering community. Although this method allows inclusions to have a certain degree of interaction, it is still not suitable for a medium with highly concentrated disk inclusions. Norris (1985), Avellaneda (1987), Berryman and Berge (1996) introduced a differential effective medium model. Kachanov et al. (1994) analyzed different effective medium models, and concluded that the Mori-Tanaka model can give a more consistent result than self-consistent model or differential models.

Effective medium theory can be used to calculate the dry frame modulus. Based on the critical porosity model, Niu et al. (2010) utilized experimental data to invert critical porosity, pore fluid and dry frame elastic parameters. Besides, inclusion-based effective medium theory can also predict the effect that different pore shapes have on the dry frame modulus. Assuming shaly sandstones contain two kinds of pores, Xu and White (1995) used the Kuster-Toksöz model to calculate dry frame modulus, and then predicted fluid saturated case with the Gassmann equation. Taking pore shape into account in actual sandstones, Vernik (1997) used Kanchanov's 2-D Mori-Tanaka model to analyze dry rock experimental data.

In this paper, we mainly employed the Mori-Tanaka model (MT) to analyze the tight sandstone experimental data from central Sichuan. Firstly, matrix parameters are obtained from velocity empirical relations, and then, the results predicted by Mori-Tanaka model (MT) with different pore shapes are compared with the experimental data. Eventually, the effects of matrix modulus and pore shape are comprehensively discussed.

# Theoretical model

Based on the strain and stress relationships between the composite material and its constituents, Berryman and Berge (1996) deduced that

$$\sum \upsilon_i (\mathbf{L}_i - \mathbf{L}^*) e_i = 0, \tag{1}$$

where the superscript * indicates the composite and the subscript i refers to the ith constituent. $\upsilon_i$ is the $i$th constituent volume fraction. $\mathbf{L}$ is the 6 × 6 stiffness matrix and $e$ is the strain.

Eshelby (1957) considered that all ellipsoidal inclusions in the composite had uniform strain, which could mathematically link the host material strain and the inclusions strain together. For any ellipsoidal inclusion, Wu (1966) subsequently proposed the tensor $\mathbf{T}^{hi}$ relating the strain in the host to the strain in the inclusion based on

$$e_i = \mathbf{T}^{hi} e_h, \tag{2}$$

where superscript $h$ represents the host. The isotropic form of $\mathbf{T}^{hi}$ can be written as

$$(\mathbf{T})_{mnpq} = \frac{1}{3}(P - Q)\delta_{mn}\delta_{pq} + \frac{1}{2}Q(\delta_{mp}\delta_{nq} + \delta_{mq}\delta_{np}). \tag{3}$$

Specific inclusions $P$ and $Q$ are described by Mavko et al. (1998) and Berryman and Berge (1996).

Based on Wu's (1966) strain relation, Berryman and Berge (1996) defined the strain in a reference material to the strain in each constituent as the linear relation

$$e_i = \mathbf{G}^{ri} e_r, \tag{4}$$

where superscript $r$ denotes the reference material and $\mathbf{G}^{ri}$ is the tensor which connects the strain in each constituent and the strain in reference material. Substituting (4) into (1) yields the equation

$$\sum \upsilon_i (\mathbf{L}_i - \mathbf{L}^*) \mathbf{G}^{ri} e_r = 0. \tag{5}$$

To get the Mori-Tanaka approximation from equation (5), we assume that the composite is a host material with inclusions and choose the host to serve as the reference material, i. e., $r \to h$, then, let $\mathbf{G}^{hi} \approx \mathbf{G}^{ri}$, and we get

$$\sum \upsilon_i (\mathbf{L}_i - \mathbf{L}^*_{\mathrm{MT}}) T^{hi} = 0. \tag{6}$$

The corresponding bulk and shear modulus can be written as

$$\begin{cases} \sum \upsilon_i (K_i - K^*_{\mathrm{MT}}) P^{hi} = 0 \\ \sum \upsilon_i (\mu_i - \mu^*_{\mathrm{MT}}) Q^{hi} = 0 \end{cases}, \tag{7}$$

where $P^{hi}$ and $Q^{hi}$ are the parameters associated with host modulus, inclusion modulus, and inclusion shape.

## Rock physics measurements

The tight sandstone reservoirs in central Sichuan mainly are distributed in the Xujiahe formation which was deposited in a fully developed fluvial delta-lake environment. From the bottom to up, the Xujiahe formation can be divided into six lithology sections. Xu-1, Xu-3 and Xu-5 are source rock formations, gas generated from these formations concentrates in reservoirs Xu-2, Xu-4 and Xu-6. In the long geological history, the Xuejiahe formation has experienced a series of digenesis, such as mechanical compaction, pressure solution, cementation, and dissolution, which result in the high heterogeneity of the reservoirs (Zhu et al., 2009). Sandstone reservoirs in the Xujiahe formation are very tight, and generally are featured with low porosity and permeability or ultra-low porosity and permeability.

All the samples we used are from the Xu-6 formation in well GuangAn101. Thin section analysis showed that the mineralogy, rock texture and pore structure of these samples have the following features: (1) sandstones in the Xu-6 formation are quartz-rich and also include many other minerals, such as feldspar, debris, calcite cement, and so on. (2) the cementation is generally not strong, with about 5% to 6% cement, but in some samples it can reach 15% or even more. The main cement constituents are silicate, chlorite, siderite, calcite, dolomite, and so on. (3) the dissolution of feldspar and volcanic debris plays a constructive digenesis role in this area, and forms secondary pores with poor connectivity. (4) these samples contain different debris, and the sandstones with highest porosity tend to have more debris. (5) well-compacted clean sands show crack-like pores in grain margins, with the pores of most samples poorly connected and even isolated, and (6) low porosity is caused by cementation and is also related to other factors such as poor sorting, compaction, quartz recrystallization, and so on.

Porosity, density, and velocity of these samples have been measured in the laboratory, referring to Figures 1 and 2. The measurement is made under the condition of room temperature, 35 MPa effective pressure, and 10 MPa pore pressure. The density and the bulk modulus of the $CO_2$ water used as pore fluid, are 1.02g/cm$^3$ and 2.505 GPa, respectively. The porosity of these sandstone samples ranges from 0.02 to 0.14, and generally P- and S-wave velocities decrease with the increase of porosity. Wet rock P-wave velocity is much larger than that of dry rock (Figure 1a) with the absolute difference about 0.2 to 0.6 km/s and the relative difference is over 7.7 %. The low porosity sandstone sample velocities increase more evidently after water saturated, which means that they contain more crack-like soft pores with poor connectivity, and P-wave velocity is more sensitive to water saturation. The absolute S-wave velocity difference between wet and dry samples is lower than 0.1 km/s, and the relative difference is less than 1.5%. The low porosity sandstone sample S-wave velocities increase after water saturated, which is contrary to the result predicted by the Gassmann equation. In the high frequency Kuster-Toksöz model (Kuster and Toksoz, 1974), shear modulus will increase with water saturation from a dry state, however, only crack-like soft pores can lead to increase in S-wave velocity. In Figure 1 we see two samples (triangles) which have much higher velocities that obviously deviate from the general velocity trend. Detail lithology investigation showed that the two samples have high cementation, poor sorting, and coarse grain segments. Comparing with velocity, the

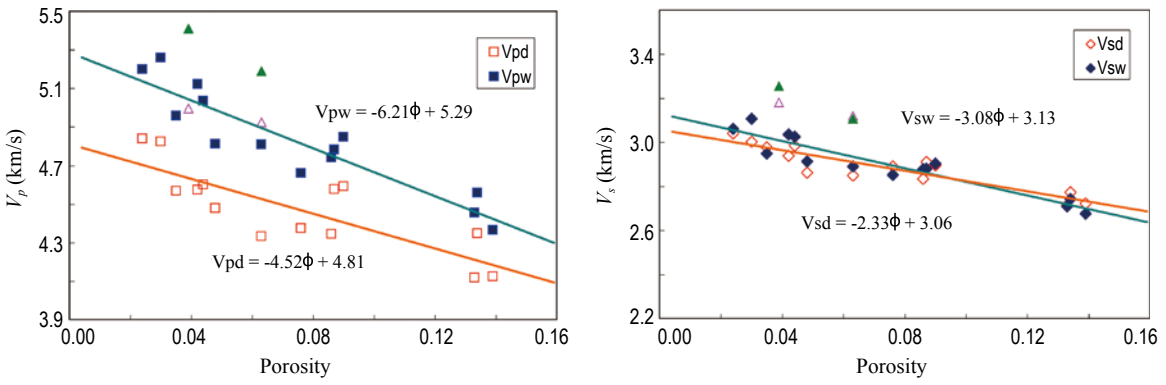


(a) P-wave velocity (b) S-wave velocity

**Fig.1 Plot of velocity versus porosity for dry (open symbols) and water saturated ( filled symbols) samples from central Sichuan.** The solid lines are empirical fits to the data and triangles represent anomalous data points.

variation of density versus porosity is simpler. Figure 2 shows dry rock density decreases linearly with the porosity increase.

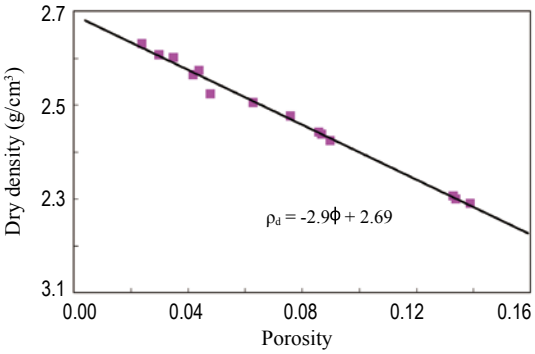


**Fig.2 Plot of density versus porosity for dry samples from central Sichuan.**
The filled squares are the measured data points and the solid line is the fitting line.

# Theoretical estimates of elastic properties

In this section, we employ the MT model to theoretically calculate the dry frame modulus, and then compare the results with the measured data. Because of velocity dispersion, the measured water saturated rock data at ultrasonic frequencies can not be properly described by this model (Ba et al. 2008; Ba et al., 2011). Before calculation with MT model, we need to know the elastic parameters of rock matrix, fluid properties, and pore shape.

## Matrix elastic parameters

The lithological analysis showed that high feldspar and siliciclastic content have some correlation with high porosity, while low porosity sandstones tend to contain more calcite and other heavy minerals. The increase of feldspar and siliciclastic content can result in the reduction of rock matrix modulus and density, whereas calcite and other heavy minerals can cause ascension of modulus and density, which means that matrix modulus and density will decrease with porosity increase.

The matrix elastic parameters can be theoretically calculated by Voigt average when each mineral's content in sandstones is known. However, the sandstone mineral composition in this region is complicated and the content of each mineral is not available, so the matrix elastic parameters can only be obtained by other methods. Vernik (1994; 1997) divided siliciclastic rocks into several lithology groups and obtained their matrix velocity by linear velocity regression for each lithology group, then converted it into matrix modulus. Under the ideal circumstances, for the rocks with the same lithology, the velocity versus porosity trend, whether dry or water saturated rock, will join at zero porosity and this point is corresponds to the matrix elastic parameter. However, because of lithology and pore geometry variation in the real cases and the effects of fluid and wave dispersion, and measurement errors, this point may be not visible in measured data.

Density linear regression of dry rock indicates that the matrix density $\rho_{m0}$ at zero porosity is 2.69 g/cm$^3$. In Figures 1a and 1b, whatever P-wave or S-wave velocity, the dry rock velocity regression line (using all the samples) does not intersect with that of water saturated rock at zero porosity. Figure 1 shows that the velocity versus porosity trend changes when porosity is below 0.07, which may be relevant to the matrix composition and pore geometry variations. In consideration of this case, we only choose low porosity sandstone velocity

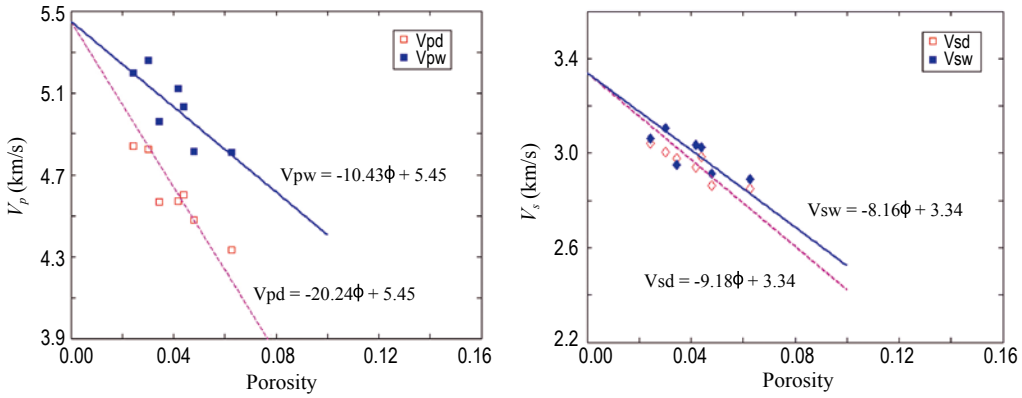


(a) P-wave velocity (b) S-wave velocity

**Fig.3 Matrix modulus obtained by linear velocity regression of part low porosity sandstones.**
The dashed and solid lines represent the linear regression for dry and water saturated samples.

data points for linear regression, and assume the dry and wet rock regression lines intersect at zero porosity. The measurement points with porosity below 0.07 are selected for linear regression (see Figure 3), and the resulting matrix P- and S-wave velocities at zero porosity are 5.45 km/s and 3.34 km/s, respectively. Combining with the previous matrix density and velocity, matrix bulk modulus $K_{m0}$ and shear modulus $\mu_{m0}$ at zero porosity are calculated as 39.89 GPa and 30.01 GPa, respectively. Normally the bulk modulus of pure quartz is 36.5 to 37.9 GPa and shear modulus is 44 to 45.6 GPa (Mavko et al., 1998). Because the sandstones in this area contain feldspar, debris, clay, calcite cement and other minerals, the calculated matrix modulus deviate from that of pure quartz, but it is similar to Han's results (Han, 1986).

## Pore shape analysis

The zeros porosity matrix modulus in the previous section will be taken as a basic parameter for pore shape analysis. Because the matrix modulus and fluid properties are known, pore shape is the only thing we want to know. Pore structure in actual rock is very complicated and pore shapes are usually irregular and various, so in theoretical calculation these pores should be properly approximated.

First, the experimental data were compared with theoretical predictions of some simple pore shapes. The pore shape is set as spheres, needles and pennies respectively (Mavko et al., 1998; Berryman and Berge, 1996; Berryman, 2006), and then we use the MT model to calculate the dry and water saturated rock moduli. Figure 4 shows the dry and water saturated rock moduli predicted by the MT model with sphere, needle and penny shape pores. Solid, dashed, and dotted lines represent the predicted values for sphere, needle and penny shape pores, respectively. For sphere and needle shapes with large aspect ratios, the dry rock bulk modulus is very close to that of wet rock (Figure 4a) and the shear moduli even overlap (Figure 4b), but these moduli are higher than the experimental results. However, for penny shapes with low aspect ratio, the predicted modulus versus porosity trend basically agrees with the experimental results, which illuminate that these sandstone samples contain crack-like soft pores.

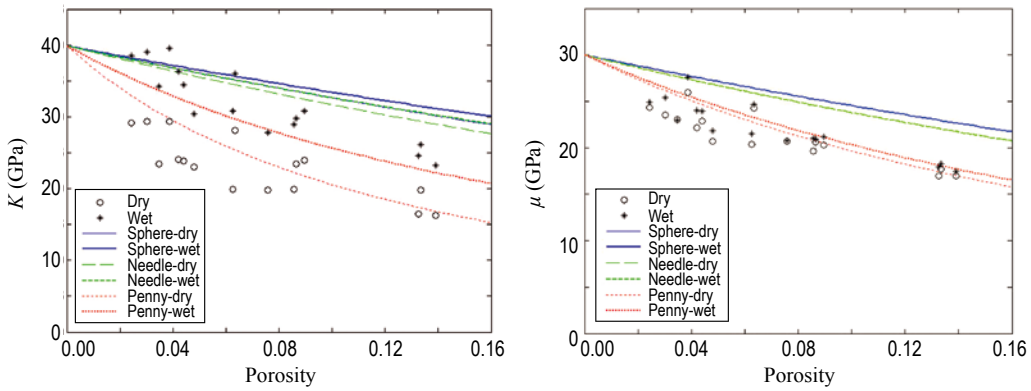


(a) Bulk modulus (b) Shear modulus

**Fig.4 Dry and water saturated rock moduli predicted by the MT model with sphere, needle and penny shaped pores.**
Circles and asterisks represent measured data of dry and water saturated rock. Solid, dashed and dotted lines represent the predicted value of sphere, needle and penny shape pores, respectively.

Based on preliminary observations of experimental data and comparison with some pore shapes, it is proven that these sandstone samples contain crack-like soft pores. If the pore shape is equivalent to ellipsoidal (Berryman, 1980; Xu and White, 1995), the pore shape variation can reflected by the aspect ratio. We assume the matrix modulus of these sandstone samples is constant, and let the matrix bulk and shear moduli equal to 39.89 GPa and 30.01 GPa respectively. Figure 5 shows the comparison between the experimental data and dry frame modulus predicted by the MT model when the pore aspect ratio is equal to 0.05, 0.09 and 0.13 respectively. In Figure 5, the effective aspect ratio of most rock samples is between 0.05 and 0.13, the aspect ratio for low porosity sandstone samples is about 0.05, and that of high porosity sandstone samples is around 0.09. For bulk and shear moduli, the pore aspect ratio range and the trend varied with porosity are consistent, which illustrates that the pore shapes are indeed change with porosity, the pore aspect ratio increases with increasing porosity.

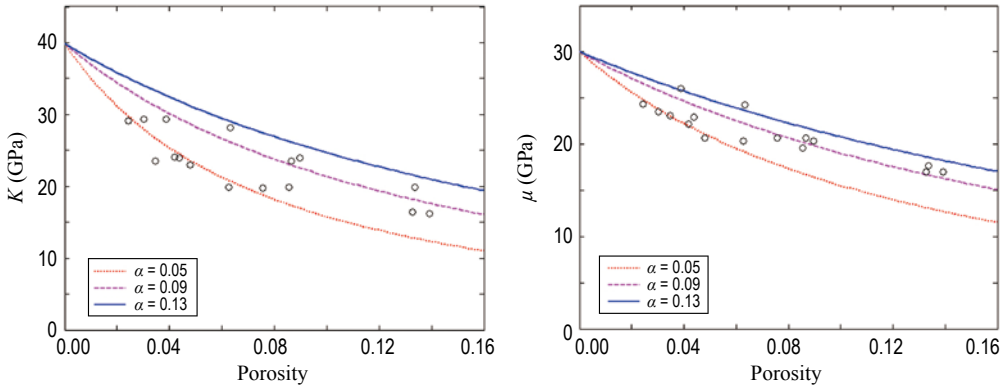


(a) Bulk modulus (b) Shear modulus

**Fig.5 Comparison between experimental data (circles) and dry frame modulus predicted by the MT model with different pore aspect ratios.**

Solid lines denote pore aspect ratio is equal to 0.13, dashed lines are 0.09, and dotted lines are 0.05.

## Comprehensive discussion

For tight sandstones, the matrix formed by mineral grains and pore fluid can be taken as host and inclusion respectively. Therefore, equation (7) is the function for matrix modulus, fluid modulus, porosity, and pore shape. We will just discuss the dry frame modulus here, and let pore shape be equivalent to ellipsoidal, so the KT model can be written as following form

$$\begin{cases} K_{\mathrm{dry}} = F(K_{\mathrm{m}}, \mu_{\mathrm{m}}, \alpha, \phi) \\ \mu_{\mathrm{dry}} = G(K_{\mathrm{m}}, \mu_{\mathrm{m}}, \alpha, \phi) \end{cases}, \tag{8}$$

where $K_{\mathrm{m}}$ and $\mu_{\mathrm{m}}$ represent bulk bulk and shear moduli respectively, and $\alpha$ is pore aspect ratio.

Actually, $K_{\mathrm{m}}$, $\mu_{\mathrm{m}}$ and $\alpha$ will change with porosity. However, at present, the matrix modulus and pore aspect ratio can not be measured directly like porosity, so it is not easy to get the relationship between porosity and pore aspect ratio.

The matrix modulus of the sandstone samples used in this study should not change too much for their main composition mineral is quartz. First, assuming the rock matrix shear modulus is constant, we can study the effects of the matrix bulk modulus and pore aspect ratio on the dry frame. Here, the matrix shear modulus is set to 30 GPa, the matrix bulk modulus takes values of 37, 40, and 43 GPa, and pore aspect ratio values are 0.05, 0.09, and 0.13. We compared the dry frame moduli predicted using the MT model with the experiment data (see Figure 6). From the Figure 6, we see that although the matrix bulk modulus are different, the pore aspect ratio for low porosity sandstones is remain about 0.05, while that of high porosity sandstones is about 0.09 (Figure 6a). The shear modulus predicted with the same pore aspect ratio and different matrix bulk moduli fall together (Figure 6b), which means that dry frame shear modulus is not sensitive to the variation of matrix bulk modulus.

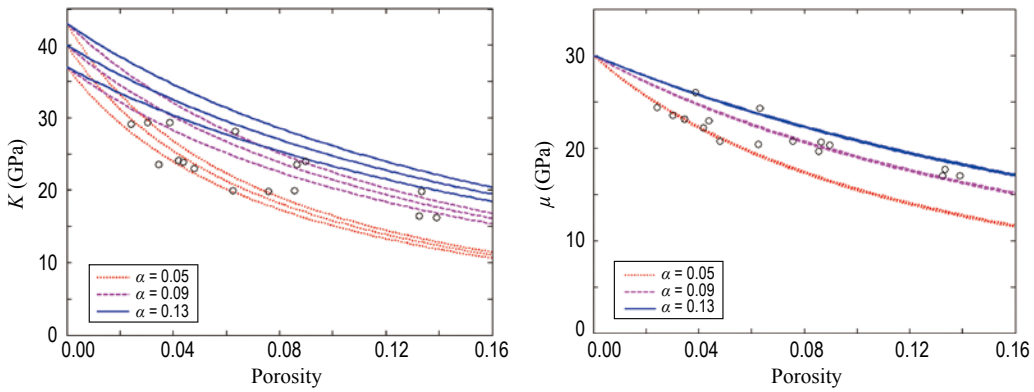


(a) Bulk modulus (b) Shear modulus

**Fig.6 Dry frame modulus predicted using the MT model with different matrix bulk moduli and pore shape and compared with the actual experimental data.**

For another case, we can evaluate the effect of matrix shear modulus and pore aspect ratio upon dry frame assuming the rock matrix bulk modulus is constant. The matrix bulk modulus is set to 40 GPa, matrix shear

modulus takes values of 29, 30, and 31 GPa and pore aspect ratio values are 0.05, 0.09, and 0.13 respectively. The MT model was used to predict the dry frame modulus and the predicted results are compared to the experimental data (see Figure 7). The bulk modulus curves predicted based on the different matrix shear moduli almost overlap together in Figure 7a, which shows that dry frame bulk modulus is not sensitive to the variation of matrix shear modulus, whereas a small matrix shear modulus change can also affect the dry frame shear modulus ( see Figure 7b).

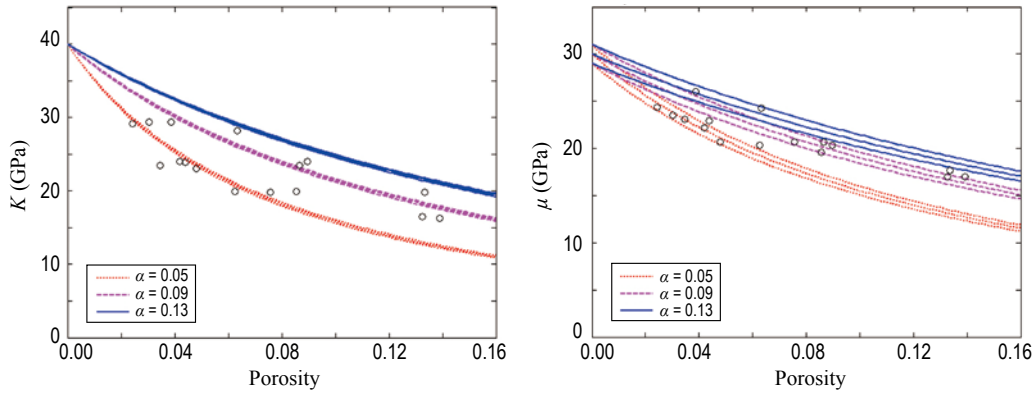


**Fig.7 Dry frame modulus predicted using the MT model with different matrix shear moduli and pore shape and compared with the experimental data.**

Both matrix modulus and pore shape have an effect on the trend that dry frame modulus varies with porosity. Based on the former observation, we conclude that both the measured point distribution of dry frame bulk modulus and shear modulus are only relevant to matrix bulk modulus and pore aspect ratio when mineral composition of rock changes little and measurement error can be neglected. Pore aspect ratio is the common factor that affects dry frame bulk modulus and shear modulus, which can cause consistent modulus variations. The trend that modulus varies with porosity in tight sandstones in this region is generally caused by the increase of effective aspect ratio, while the partly scattered points are related to mineral composition variation.

## Conclusions

Tight sandstone samples from central Sichuan have high heterogeneity, very low porosity and low permeability. The pores can be micro-structurally taken as the inclusions embedded in the rock matrix. We adopted the Mori-Tanaka model to analyze the observed velocity data of tight sandstone samples in the dry case, and the results show that:

1.The experimental data is close to the result theoretically predicted by low pore aspect ratio. The effective pore aspect ratio of most rock samples is between 0.05 and 0.13, and increases with porosity.

2. Matrix modulus and pore shape both have effect on dry frame modulus. Under the condition of small change in mineral composition, the dry frame bulk modulus is not sensitive to matrix shear modulus variation, and dry frame shear modulus is also not affected by matrix bulk modulus. Pore aspect ratio is a common factor that affects both dry frame bulk modulus and shear modulus, which can cause their consistent variation.

3. For these sandstone samples, the trend that modulus varies with porosity is generally caused by increase in effective pore aspect ratio, while local scattered points may be related to mineral composition variation.

Note that before performing pore shape analysis, we obtained the matrix parameters from the linear regression of velocity data with the prerequisite of no change in mineral composition and pore structure. This may not be possible for actual rock. However, we can intercept the low porosity sandstone measurements to approach it. For assuring the analysis reliability, we also considered the comprehensive matrix modulus and pore shape effect. Matrix modulus and Density have some relationships with porosity, which can be used to building a simpler and more practical model. This is a topic that we will research as the next step.

## References

Avellaneda, M., 1987, Iterated homogenization, differential effective medium theory and application: Commun. Pure

Appl. Math., **40**, 527 – 554.

Ba, J., Cao, H., Yao, F. C., Nie, J. X., and Yang, H. Z., 2008, Double-porosity rock model and squirt flow in the laboratory frequency band: Applied Geophysics, **5**(4), 261 – 276.

Ba, J., Carcione, J. M., and Nie, J. X., 2011, Biot-Rayleigh theory of wave propagation in double-porosity media: Journal of Geophysical Research, **116**, B06202 1 – 12.

Berryman, J. G., 1980, Long-wavelength propagation in composite elastic media II. Ellipsoidal inclusions: J. Acoust. Soc. Am., **68**(6), 1820 – 1831.

Berryman, J. G., 2006, Effective medium theories for multicomponent poroelastic composites: Journal of Engineering Mechanics, **132**(5), 519 – 531.

Berryman, J. G,, and Berge, P. A., 1996, Critique of two explicit schemes for setimating elastic properties of multiphase composites: Mechanics of Materials, **22**, 149 – 164.

Budiansky, B., 1965, On the elastic moduli of some heterogeneous materials: J. Mech. Phys. Solids, **13**, 223 – 227.

Han, D. H., 1986, Effects of porosity and clay content on acoustic properties of sandstones and unconsolidated sediments: PhD Thesis, Stanford University.

Hill, R., 1965, A self-consistent mechanics of composite materials: J. Mech. Phys. Solids, **13**, 213 – 222.

Kachanov, M., Tsukrov I., and Shafiro B., 1994, Effective moduli of solids with cavities of various shapes: Appl. Mech. Rev., **1**, S151 – S174.

Korringa, J., Brown, R. J. S, Thompson, D. D., and Runge, R. J., 1979, Self-consistent imbedding and the ellipsoidal model for porous rocks: J. Geophys. Res., **84**, 5591 – 5598.

Kuster, G. T., and Toksoz, M. N., 1974, Velocity and attenuation of seismic waves in two-phase media: Part I. Theoretical formulations: Geophysics, **39**(5), 587 – 606.

Mavko, G., Mukerji, T., and Dvorkin, J., 1998, The rock physics handbook: Tools for seismic analysis in porous media: Cambridge University Press, New York.

Mori, T., and Tanaka, K., 1973, Average stress in matrix and average elastic energy of materials with misfitting inclusions: Acta Metallurgica, **21**(5), 571 – 574.

Niu, B. H., Sun, C. Y., Yan, G. Y., Yang, W., and Liu, C., 2010, Numerical calculation method for getting critical point, pore fluid and framework parameters of gas-bearing media: Chinese J. Geophys. (in Chinese), **53**(6), 1495 – 1501.

Norris, A. N., 1985, A differential scheme for the effective moduli of composites: Mechanics of Materials, **4**, 1 – 16.

Vernik, L., 1994, Predicting lithology and transport properties from acoustic velocities based on petrophysical classification of siliciclastics: Geophysics, **59**(3), 420 – 427.

Vernik, L., 1997, Predicting porosity from acoustic velocities in siliciclastics: A new look: Geophysics, **62**(1), 118 – 128.

Vernik, L., and Kachanov M., 2010, Modeling elastic properties of siliciclastic rocks: Geophysics, **75**(6), E171 – E182.

Wu, T. T., 1966, The effect of inclusion shape on elastic moduli of a two-phase material: Int. J. Solids Structures, **2**, 1 – 8.

Xu, S., and White R. E., 1995, A new velocity model for clay-sand mixtures: Geophysical Prospecting, **43**, 91 – 118.

Zhu, R. K., Zou, C. N., Zhang, N, Wang, X. S., Cheng, R., Liu, L. H., Zhou, C. M., and Song, L. H., 2009, Diagenetic fluids evolution and genetic mechanism of tight sandstone gas reservoirs in Upper Triassic Xujiahe Formation in Sichuan Basin, China: Science in China Series D: Earth Sciences (in Chinese), **39**(3), 327 – 339.

**Yan Xin-Fei** received his MS degree from China University of Geoscience (Beijing) in 2006. Now he is studying for his PhD degree in geophysical prospecting and information technology at the Research Institute of Petroleum Exploration and Development. His current research interests include AVO hydrocarbon detection, and rock physics experiments and applications.